doi:10.1017/S1431927617007942
Microsc. Microanal. 23 (Suppl 1), 2017

Advances in Elemental Electron Tomography for the State-of-the-art Semiconductor Devices and Circuits Characterization and Failure Analysis

B. Fu[1], M Gribelyuk[1], Frieder H. Baumann[1], C. Fang[1], Wayne Zhao[1], E. Chen[1], I. Brooks[1]

[1.] GLOBALFOUNDRIES, 400 Stone Break Rd Extension, Malta, NY, USA 12020

Electron tomography is a well-established technique that has long been used in life science for 3-dimensional (3D) imaging of amorphous materials. Its application to semiconductor materials and devices is limited until the advent of high-angle-annular-dark-field scanning transmission electron microscopy (HAADF-STEM) technique, which extends to the 3D structure characterization of (partially) crystalline semiconductor materials [1]. Such a 3D characterization of devices is essential as the semiconductor manufacturing industry has implemented 3D structures like finFet devices, because conventional 2-dimensional (2D) TEM cross-sectional view is no longer adequate due to "projection effect" [2]. More importantly, the heterogeneous semiconductor structure often makes 3D chemical maps required to understand the true elemental distribution in device and circuit characterization and failure analysis. However, the application of the traditional manual elemental tomography analysis in manufacturing foundries is usually precluded due to the fact that it usually takes days or even weeks to obtain results, while the analysis turn-around time is critical for a high-volume semiconductor manufacturing foundry. Thus, few studies [3, 4] have been tried to characterize semiconductor devices in manufacturing foundries using elemental tomography.

Recent development of X-rays detector systems with higher collection efficiency has made it possible to collect EDS elemental maps with substantially improved S/N within a few minutes [5]. That not only enables EDS elemental tomography to meet the analysis turn-around time requirement in semiconductor industry, but, more importantly, drastically reduces the electron radiation damage during data collection. In this study, a fully automated EDS tomography system is used for data collection: a tilt series with about 30 EDS elemental maps usually takes less than 3 hours. After data collection, batch processing allows all elemental maps to be background subtracted, deconvoluted, aligned, and reconstructed. This greatly reduces the hitherto tedious and time-consuming manual processing, alignment, and reconstruction work of each individual elemental map.

A few 3D EDS elemental tomography for semiconductor characterization and failure analysis application examples will be presented using the aforementioned system. Figure 1 depicts a particle observed in the S/D region. Previous STEM z-contrast tomography showed the particle is present prior to NiSi formation and the composition of the particle mainly contains a mixture of silicon oxide and nitride [6]. With 3D EDS elemental tomography, it can be shown that the particle originates as a silicon oxide core, and then wrapped with silicon nitride downstream in the fabrication process.

In figure 2, TEM images of a defect in 3D fin-FET technology are presented both in planar and cross-section direction at the same location. Simultaneously, STEM and EDS elemental tomography is also applied to study the same defect. The result shows that with tomography the defect origination location can be revealed, and it provides more information that can be obtained by the combination of analysing the planar and cross-section samples.

The presented results illustrate unique opportunities of applying elemental tomography for characterization and failure analysis of semiconductor devices to better understand the failure mechanism for yield improvement [7].

References:

[1] P. A. Midgley, M. Weyland, Ultramicroscopy **96** (2003), p. 413.
[2] David B. Williams and C. Barry Carter in “Transmission Electron Microscopy”, 2nd Edition, (Springer, New York, NY) p.9.
[3] J. Zhang *et al*, Microscopy and Microanalysis **21**(S3) (2015), p. 2333.
[4] F. Baumann *et al*, Microscopy and Microanalysis **22**(S3) (2016), p. 280.
[5] R. Pantel, Ultramicroscopy, **111** (2011), p. 1607.
[6] B. Fu *et al*, Microscopy and Microanalysis **22**(S3) (2016), p. 326.

[7] The authors acknowledge R. Newkirk, B. Popielarski, and N. LaManque for preparing the TEM samples.

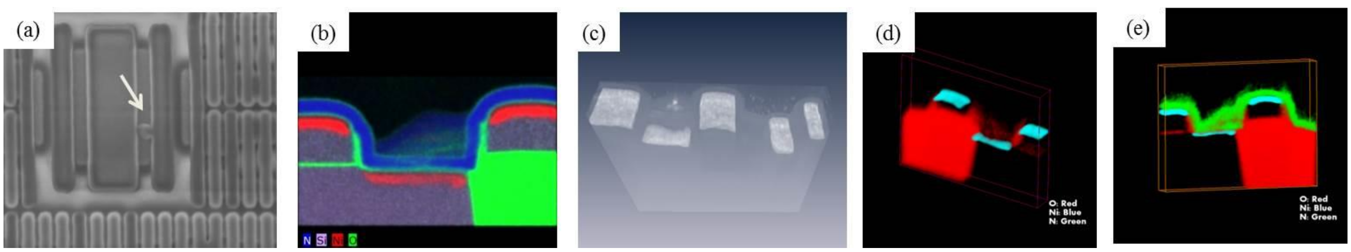

Figure 1. (a) Top-down SEM image of the defect location (arrowed); (b) Cross-section EDS elemental map of the defect; (c) STEM tomography voltex visualization of the particle; (d),(e) EDS elemental tomography of the defect.

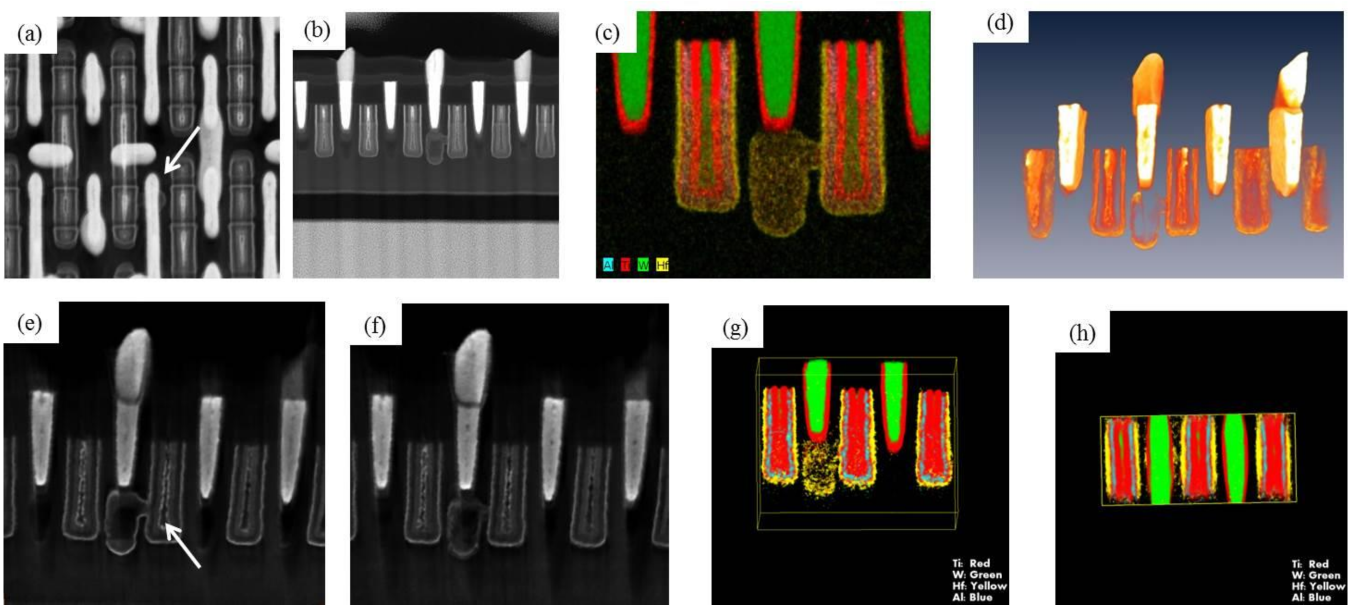

Figure 2. (a) Planar-TEM view of the sample; (b) Converted cross-section view of the planar sample in (a); (c) Cross-section EDS elemental map of the defect; (d) STEM tomography voltex visualization of the defect; (e), (f) Reconstructed OrthoSlice of the defect; (g),(h) EDS elemental tomography of the defect.